

Hyperconjugative Interactions in Permethylated Siloxanes and Ethers: The Nature of the SiO Bond

Frank Weinhold and Robert West*

Department of Chemistry, University of Wisconsin, Madison Wisconsin 53706, United States

S Supporting Information

ABSTRACT: The paradoxically low basicity (despite high anionicity) of oxygen in the characteristic Si–O–Si linkages of silicone polymers is investigated with hybrid density functional and natural bond orbital (NBO) computational methods, extending a previous study of idealized disiloxane and dimethyl ether parent species to fully methylated derivatives that more faithfully model the silicone polymers of industrial and environmental importance. Despite the complicating distortions of the sterically crowded di-*t*-butyl ether “analog”, the physical picture of enhanced hyperconjugative (resonance-type) delocalization in Si–O vs C–O bonding is essentially preserved (and indeed accentuated) in permethylated species. NBO-based orbital overlap diagrams are employed in conjunction with structural, hybridization, and polarity descriptors to illustrate the subtle phase-matching relationships that confer superior enthalpic and entropic stability (and low basicity) on permethylated Si–O–Si linkages. Our results challenge both ionic models of Si–O bonding and conventional electrostatic-type models of H-bonding and acid–base reactivity.



INTRODUCTION

Silicones, polysiloxane polymers, are an inescapable part of modern life. To cite a few examples: Silicone rubbers are important as electrical insulating materials, building sealants, hydraulic lines, and implantable medical materials. Lower molecular weight silicones are widely used in shampoos, hair conditioners, and other personal care products. The properties of silicones which render them so useful all depend on the silicon–oxygen bonds which form the backbone of these polymers.^{1,2} In view of the importance of silicon–oxygen bonding in siloxanes, it is striking that the nature of the silicon–oxygen bond is not well understood and is in fact controversial.³

The desirable properties of silicones result in large part because the oxygen atoms, despite their expected high anionicity when bonded to silicon, are quite weakly basic. The higher anionicity of oxygen in Si–O–Si vs C–O–C bonding could be anticipated from freshman chemistry concepts (and confirmed by high-level atomic charge assignments), but the usual electrostatic picture of intermolecular interactions would then suggest *higher* rather than weaker basicity. Nevertheless, the weak basicity of polysiloxanes was first observed many years ago^{4–6} and has been nicely confirmed by a recent careful study.⁷ Indeed, the weakly basic oxygens render the polysiloxanes water repellent and resistant to solvolysis, properties that underlie their many industrial applications.

What, then, is the reason for the low basicity of siloxanes? Two models are currently employed to answer this question. One holds that the basicity is reduced by hyperconjugative delocalization from the lone pairs of oxygen into adjacent antibonding σ^*_{SiC} orbitals (significantly enhanced by the low electronegativity of Si compared to analogous $n_{\text{O}} \rightarrow \sigma^*_{\text{CH}}$

delocalization in ethers).^{3,8–12} In a diametrically opposed view based on calculation of the electron localization function (ELF), the Si–O bond is regarded as essentially ionic.^{13,14} Further clarification of the nature of Si–O bonding in siloxanes thus seems warranted.

In an earlier paper³ we investigated the Si–O chemical bonding in disiloxane ($\text{H}_3\text{Si–O–SiH}_3$, DSE) compared with the isostructural compound dimethyl ether ($\text{CH}_3\text{–O–CH}_3$, DME) employing natural bond orbital (NBO) methods.¹⁵ Hyperconjugative $n_{\text{O}} \rightarrow \sigma^*_{\text{XH}}$ electron release from the oxygen lone pairs into the antibonding X–H orbitals takes place for both compounds. However this interaction is greater for DSE than for DME, in spite of the larger distance between the interacting orbitals in the silicon than in the carbon compound. The larger hyperconjugative interaction and consequent greater electron withdrawal from oxygen lone pairs make the DSE less basic than DME, despite higher overall anionicity on O bonded to Si.

This bonding model might be extended to silicone materials other than DSE. However in silicones, the silicon atoms are bonded to carbon (usually methyl) groups, rather than to hydrogens. Thus it seemed important to examine the bonding in a compound more representative of silicone structures. We now report NBO calculations on the hexamethylated analogs, hexamethyldisiloxane (HMDSE), the smallest member of the polydimethylsiloxane series, and di-*t*-butyl ether (HMDME). For consistency in all comparisons, we employ the same B3LYP/aug-cc-pVTZ theoretical level which was found to give excellent agreement with best available theoretical and experimental results for parent DME, DSE species.³

Received: January 3, 2013

Published: March 27, 2013

RESULTS AND DISCUSSION

Structural Properties. Figure 1 displays ORTEP views of the calculated equilibrium structures for the four considered

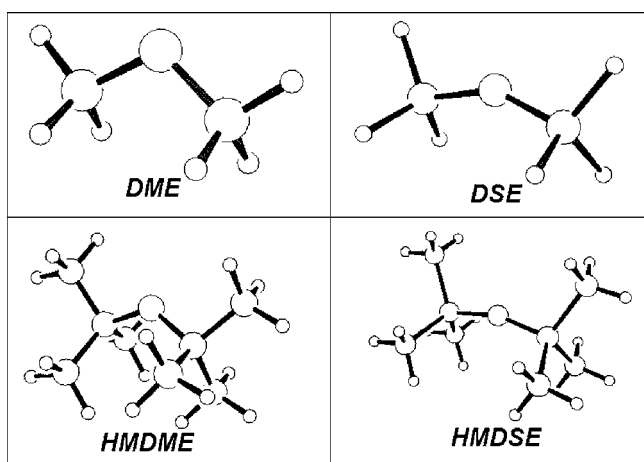


Figure 1. Optimized structures of ethers (left) and siloxanes (right) considered in this work, showing the distinctive “staggered” (C_2) geometry of HMDME in contrast to the “eclipsed” (C_{2v}) geometry of other species.

species, and Table 1 compares numerical values of various structural properties of interest. As seen at the lower-left of Figure 1, HMDME exhibits an anomalous twisted (“staggered”) geometry that presumably reflects the significantly higher steric strain of bulky substituent *t*-butyl groups on the skeletal geometry of ethers compared to siloxanes.

The entries of Table 1 confirm the picture of severe steric strain in HMDME compared to other species. Permethylated leaves the Si–O bond length of HMDSE unperturbed compared to DSE but stretches the corresponding C–O bond length of HMDME by 0.04 Å compared to DME. Most strikingly, permethylation widens the C–O–C bond angle of DME by more than 15° in HMDME (compared to ~6° increase in HMDSE). Steric cramping in the ethers is also evident in the low-frequency torsional vibrations (fifth row of Table 1), which are seen to be 5–7 times higher than those for corresponding siloxanes, thus conferring significant entropic advantage on the latter. The positive ν_i values also further show that the calculated structures are all stable equilibrium species.

The final row of Table 1 shows NBO estimates (pairwise steric exchange E_{PWX} from natural steric analysis)¹⁶ of steric repulsions for proximal H···H contacts. The $E_{\text{PWX}}(\text{H}\cdots\text{H})$

values confirm that such steric clashes are essentially negligible in the siloxanes but remain quite appreciable in DME and (especially) HMDME. Two strong residual H···H clashes (each estimated at 1.70 kcal/mol) remain in HMDME, despite the severe skeletal twisting, C–O stretching and C–O–C angle bending which serve to relieve steric repulsions in this species.

Figure 2 shows (pre-)NBO¹⁷ orbital overlap diagrams that depict the strongest steric H···H clashes in each species, both as surface plots and contour diagrams. The graphical images are in accord with the numerical $E_{\text{PWX}}(\text{H}\cdots\text{H})$ estimates of Table 1 that steric clashes between filled NBOs are essentially absent in the siloxanes but quite appreciable in the ethers. As shown in the upper-right panel of Figure 2, two such proximal clashes occur in the twisted geometry of HMDME, compared to the single clash in DME.

The calculated structural properties of all species appear to be in satisfactory agreement with available experimental values or best previous theoretical values. Structural determinations on HMDSE by X-ray¹⁸ and electron diffraction (ED)^{19,20} suggest a Si–O distance of ~1.63 Å, compared to our calculated value of 1.65 Å. The Si–O–Si angle, however, varies considerably depending on the method of measurement. The Si–O–Si bending potential in siloxanes is known to be very small, so the DSE bond angle can be expected to vary somewhat with temperature and phase. A 1976 gas-phase ED study reported a value of 148.0° for the Si–O–Si angle,¹⁹ but a later similar determination by Borisenko and co-workers²⁰ found 152° for this angle. Condensed phase measurements find somewhat smaller values. A solid-state X-ray diffraction investigation by Chernega and co-workers reported a value of 148.25° for the Si–O–Si angle,¹⁸ and a recent study of the vibrational spectra of liquid HMDSE was consistent with a value near 150°.²¹ Our calculated value (156.7°) is somewhat larger than these measured values but closest to the more recent gas-phase ED result.

For the carbon analog HMDME, the C–O–C angle has been measured by electron diffraction²² to be 130.8°. Molecular mechanics calculations on this molecule give a slightly smaller value, 129.0° at the MM4(r_g) level.²³ Gregerson et al.²⁴ carried out extensive ab initio and density functional calculations on the ethers (comparing their results with available experimental data) and obtained a value of 127.6° at what was considered their “best” [B3LYP/DZ+(2d,p)] theoretical estimate, very close to our value, 127.9°. The C–O–C angle in HMDSE is known to be exceptionally large compared with the same angle in ethers with smaller substituent groups, as shown by the corresponding values for DME (111.8°,²⁵ 112.6°²⁴) and methyl *t*-butyl ether (115.8°,²⁵ 118.0°²⁴). The steric origin of the

Table 1. Structural Properties of $X_3\text{RORX}_3$ Species (R = C, Si; X = H, CH_3), Showing Differences in Point Group Symmetry, R–O–R and O–R–X Bending Angles, Steric Repulsion of Proximal $\sigma_{\text{CH}}-\sigma_{\text{CH}}$ Bonds (E_{PWX}), and Lowest Vibrational Frequencies (ν_i) in Ethers and Disiloxanes

property	R = C		R = Si	
	X = H (DME)	X = CH_3 (HMDME)	X = H (DSE)	X = CH_3 (HMDSE)
point group	C_{2v}	C_2	C_{2v}	C_{2v}
R–O distance (Å)	1.41	1.45	1.65	1.65
R–O–R angle (°)	112.7	127.9	150.3	156.7
O–R–X angle (°)	107.4	102.4	110.2	107.7
lowest ν_i (cm^{-1})	207, 239, ...	74, 114, ...	29, 43, ...	11, 23, ...
$E_{\text{PWX}}(\text{H}\cdots\text{H})$ (kcal/mol)	1.06	1.70	– ^a	– ^a

^aSubthreshold for printing (<0.5 kcal/mol).

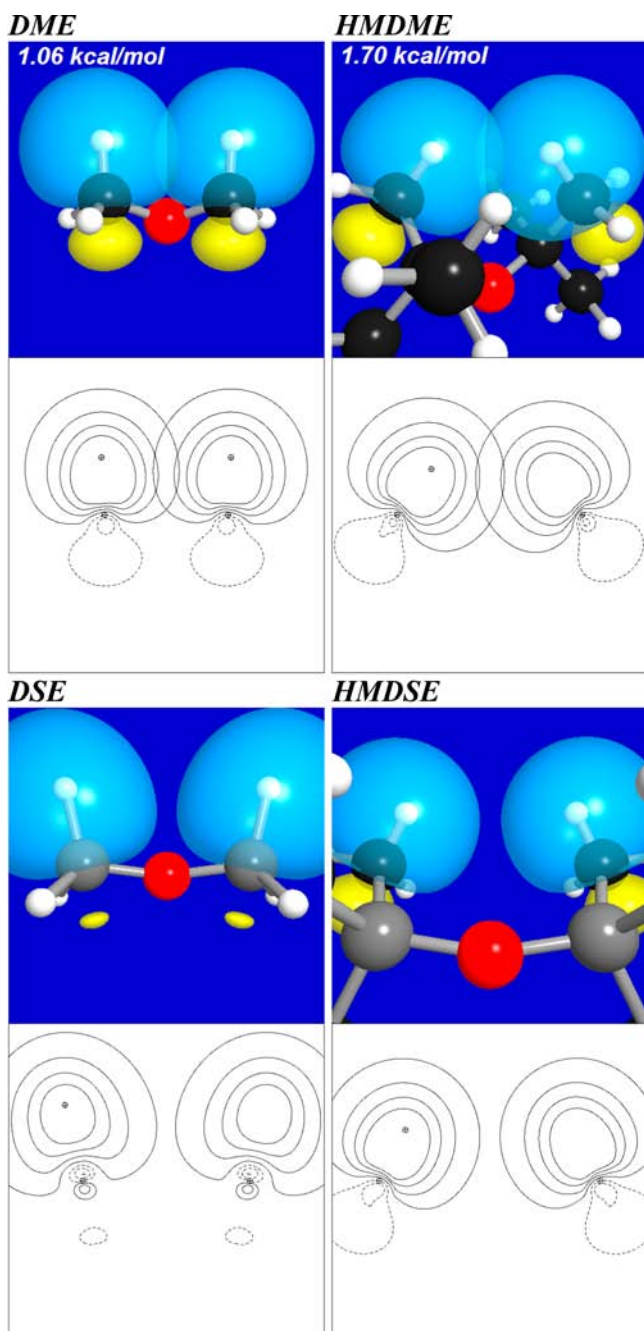


Figure 2. Proximal H...H steric interactions (and associated E_{PWX} repulsion energy; cf. Table 1) in ethers (upper) and siloxanes (lower), as compared in surface and contour plots.

exceptional HMDME distortions has been generally recognized.

The analogous experimental and theoretical comparisons for parent DME, DSE species (where much higher theoretical treatments are available) were discussed in preceding work.³ All available comparisons suggest that the adopted B3LYP/aug-cc-pVTZ computational level is quite adequate to realistically represent the polarity and hyperconjugative properties of Si–O vs C–O bonding that are the principal focus of this study.

Polarity and Hybridization Properties. Table 2 displays calculated values of various theoretical descriptors of Si–O vs C–O polarity and atomic charge distribution in siloxanes and

Table 2. Polarity Properties of X_3RORX_3 Species ($\text{R} = \text{C}, \text{Si}$; $\text{X} = \text{H}, \text{CH}_3$), Showing Differences in Bond Ionicities of OR and RX Bonds ($i_{\text{OR}}, i_{\text{RX}}$) and Natural Atomic Charge at Oxygen (Q_{O}) in Ethers and Siloxanes

property	R = C		R = Si	
	X = H (DME)	X = CH ₃ (HMDME)	X = H (DSE)	X = CH ₃ (HMDSE)
i_{OR}	0.337	0.362	0.711	0.732
i_{RX}	0.188	0.008	−0.206	−0.456
Q_{O}	−0.566	−0.633	−1.266	−1.291

ethers. The first two rows show the bond ionicity i_{AB} , defined for general σ_{AB} bond as

$$i_{\text{AB}} = |c_{\text{A}}|^2 - |c_{\text{B}}|^2 \quad (1)$$

Numerical ionicities are obtained from NBO polarization coefficients c_{A} and c_{B} for σ_{OR} or σ_{RX} bonds ($\text{R} = \text{C}, \text{Si}$; $\text{X} = \text{H}, \text{CH}_3$), with values ranging from covalent (0) to ionic (−1/+1) limits:

$$-1 \leq i_{\text{AB}} \leq +1 \quad (2)$$

The tabulated ionicity values show (as expected) that σ_{SiO} bonds are more polarized than σ_{CO} bonds, and σ_{SiX} bonds are oppositely polarized to σ_{CX} bonds, but all values remain well separated from the “extreme ionic” ($Q_{\text{O}} = -2$; $i_{\text{OR}} = +1$) limit.

For each choice of $\text{X} = \text{H}$ or CH_3 , the bond ionicities i_{OR} of O–R bonds are increased (and those i_{RX} of adjacent R–X bonds are diminished) for $\text{R} = \text{Si}$ compared to $\text{R} = \text{C}$, consistent with natural²⁶ or empirical electronegativities. Tabulated natural atomic charges (Q_{O}) of Table 2 also confirm the elementary freshman expectation that the oxygen atom of siloxanes is far more anionic than that of ethers. Permethylated species leads to increased anionicity in both cases, again consistent with qualitative electronegativity differences.

In accordance with Bent’s rule,²⁷ the increased R–O bond polarities of permethylated species lead to increased oxygen hybrid s-character and R–O–R bending angles in both ethers

Table 3. Hybridization Properties of X_3RORX_3 Species ($\text{R} = \text{C}, \text{Si}$; $\text{X} = \text{H}, \text{CH}_3$), Showing Differences in sp^{λ} Hybrid Type and % s Character of h_{O} and h_{R} Natural Hybrids, Idealized R–O–R Hybrid Angle $\Theta^{(0)}_{\text{ROR}}$, and Deviation of Actual R–O–R Angle from Ideality, $\Delta\Theta$, in Ethers and Siloxanes

species	h_{O}	% s	h_{R}	% s	$\Theta^{(0)}_{\text{ROR}}$	$\Delta\Theta$
R = C						
DME	$\text{sp}^{2.57}$	27.9%	$\text{sp}^{3.34}$	23.0%	112.9°	−0.2°
HMDME	$\text{sp}^{2.23}$	30.9%	$\text{sp}^{4.01}$	19.9%	116.6°	+11.3°
R = Si						
DSE	$\text{sp}^{1.22}$	44.9%	$\text{sp}^{3.35}$	22.7%	145.1°	+5.2°
HMDSE	$\text{sp}^{1.08}$	48.1%	$\text{sp}^{3.63}$	21.3%	157.8°	−1.1°

and siloxanes. Table 3 displays the hybrid sp^{λ} type and % s character at each center, the idealized $\Theta^{(0)}_{\text{ROR}}$ bonding angle:²⁸

$$\Theta^{(0)}_{\text{ROR}} = \cos^{-1}(-1/\lambda) \quad (3)$$

and the angular deviation from ideality, $\Delta\Theta = \Theta_{\text{ROR}} - \Theta^{(0)}_{\text{ROR}}$ for the various h_{O} and h_{R} bonding hybrids.

As seen in the first two columns of Table 3, the % s character of h_{O} natural hybrids indeed rises sharply in the siloxanes (even more sharply in HMDSE), leading to the larger $\Theta^{(0)}_{\text{ROR}}$

interhybrid bond angle predicted by Bent's rule. As seen in the final column, the actual R–O–R bond angle conforms reasonably to this predicted value except for HMDME, where steric stresses lead to appreciable C–O bond bending ($\sim 6.3^\circ$ deviations from the line of centers) at each nuclear center. Compared to DME, the greater part of the R–O–R increase in HMDME can therefore be properly attributed to steric deformation and resultant bond bending rather than Bent's rule-type rehybridization effects.

Hyperconjugative Properties. As discussed in ref 3, basicity at oxygen is strongly affected by hyperconjugative $n_{\text{O}} \rightarrow \sigma_{\text{RX}}^*$ delocalizations from in-plane (n_{O}') or out-of-plane (n_{O}'') oxygen lone pairs into vicinal antibond σ_{RX}^* NBOs that compete with the analogous intermolecular $n_{\text{O}} \rightarrow \sigma_{\text{AH}}^*$ donor–acceptor interactions that underlie acid–base reactivity.²⁹ Siloxane basicity is therefore expected to be only weakly perturbed by the structural and polarity shifts associated with permethylation, but the profound hyperconjugative differences in Si–O vs C–O bonding are expected to persist in analogous comparisons of HMDSE vs HMDME.

Table 4 displays key NBO-based descriptors of hyperconjugative loss at oxygen lone pairs, including final n_{O}' , n_{O}''

Table 4. Hyperconjugative Properties of X_3RORX_3 Species (R = C, Si; X = H, CH_3), Showing Differences in Oxygen Lone Pair (n_{O}' , n_{O}'') Occupancies (e), Net Hyperconjugative Electronic Loss (e), % Loss (relative to parent DME), and $n_{\text{O}} \rightarrow \sigma_{\text{RX}}^*$ Hyperconjugative Stabilization Energies ($E^{(2)}$; kcal/mol) for Largest Single Value ($E^{(2)}_{\text{max}}$) and Sum Total ($E^{(2)}_{\text{total}}$) of Vicinal Interaction Values in Ethers and Siloxanes

property	R = C		R = Si	
	X = H (DME)	X = CH_3 (HMDME)	X = H (DSE)	X = CH_3 (HMDSE)
occ. n_{O}'	1.968	1.952	1.926	1.917
occ. n_{O}''	1.919	1.926	1.919	1.913
hc loss	0.113	0.122	0.155	0.170
(rel. %)	(0%)	(8.0%)	(37.2%)	(50.4%)
$E^{(2)}(n_{\text{O}}' \rightarrow \sigma_{\text{RX}}^*)_{\text{max}}$	−2.48	−3.75	−5.35	−6.29
$E^{(2)}(n_{\text{O}}' \rightarrow \sigma_{\text{RX}}^*)_{\text{total}}$	−7.78	−11.92	−16.37	−20.00
$E^{(2)}(n_{\text{O}}'' \rightarrow \sigma_{\text{RX}}^*)_{\text{max}}$	−6.46	−7.55	−5.64	−5.56
$E^{(2)}(n_{\text{O}}'' \rightarrow \sigma_{\text{RX}}^*)_{\text{total}}$	−25.84	−23.84	−20.73	−21.94

occupancy and corresponding loss (“hc loss”, both in absolute terms and percentage relative to DME) from idealized double occupancy and second-order estimates $E^{(2)}$ of associated $n_{\text{O}} \rightarrow \sigma_{\text{RX}}^*$ interaction strength (kcal/mol), both for the single largest (“max”) and sum (“total”) of vicinal interactions of each type.

As shown in the third and fourth rows of Table 4, intramolecular hyperconjugative loss from oxygen lone pairs is far greater in siloxanes than in ethers, further exacerbated by effects of permethylation. The associated $E^{(2)}$ estimates (rows 5–8) also reflect these trends, particularly for the in-plane n_{O}' lone pair. As described previously for DME and DSE,³ in-plane hyperconjugative delocalizations depend strongly on R–O–R bond angle, which is intrinsically increased in siloxanes due to Bent's-type electronegativity and hybridization effects. All numerical results of Table 4 are consistent with the simple physical picture of reduced basicity in siloxanes due to

hyperconjugative depletion of oxygen lone pairs, despite expected inductive differences in the bonding skeleton that confer higher overall anionicity to Si-bound oxygen.

Figure 3a illustrates in-plane $n_{\text{O}}' \rightarrow \sigma_{\text{RX}}^*$ hyperconjugative delocalization of siloxanes vs ethers in NBO overlap diagrams (both surface and contour plots; cf. corresponding steric overlap diagrams of Figure 2). The greater strength of $n_{\text{O}}' \rightarrow \sigma_{\text{SiX}}^*$ delocalizations can be visualized from the increasingly strong “ π -type” donor–acceptor overlap as skeletal bond angle opens,³⁰ based on familiar maximum overlap concepts of covalent bonding. Figure 3b shows the corresponding overlap diagrams for out-of-plane $n_{\text{O}}'' \rightarrow \sigma_{\text{RX}}^*$ delocalizations, where siloxane and ether interactions are of comparable strength.

From comparisons of the left vs right panels of Figure 3a,b, one can see that permethylation involves the distinctive change of shape of σ_{RC}^* vs σ_{RH}^* acceptor orbitals (with an additional nodal plane between the nuclei in the former case) as well as subtle structural R–O–R and polarity shifts that alter the crucial phase matching between donor and acceptor NBOs. However, the basic differences of the parent DME vs DSE species seem to be essentially preserved in all these comparisons. Hyperconjugative delocalization is clearly an important aspect of both Si–O and C–O bonding, but particularly so in the former case.

■ SUMMARY AND CONCLUSIONS

The present work essentially confirms and amplifies the conclusions of our earlier study³ of unsubstituted DME/DSE skeletal species, despite the significant structural perturbations due to permethylation. In the ether derivatives, the steric pressures of permethylation lead to dramatic twisting, stretching, and (most importantly) C–O–C angle bending effects that somewhat complicate, but do not obscure, the NBO-based comparisons with siloxane derivatives. Compared to the corresponding ethers, permethylated siloxanes are found to exhibit even stronger evidence for the powerful effects of hyperconjugation (specifically, resonance-type delocalization of oxygen lone pairs into adjacent σ_{SiC}^* antibond orbitals) that significantly alter the structural and reactive properties of Si–O bonds compared to C–O bonds.

Although hyperconjugatively modified Si–O bonds exhibit the higher polarity to be expected from standard electronegativity considerations as well as the associated hybridization and structural changes to be anticipated from Bent's rule, our study finds no evidence for the extreme ionic picture of Si–O bonding as advocated in refs 13 and 14. Indeed, NBO-based ionicity and atomic charge descriptors offer a mutually consistent picture (and associated numerical quantification) that fits comfortably into the general framework of polar covalency, far from the ionic limit. In this sense, our results emphasize the many commonalities of C–O–C vs Si–O–Si bonding, rather than any dichotomous “covalent vs ionic” distinction between ethers and siloxanes.

The enhanced hyperconjugative interactions of permethylated siloxanes naturally imply an enhanced palette of resonance-type electro-optical properties as well as associated enthalpic stabilization and diminished reactivity. However, it is interesting to recognize that $n_{\text{O}} \rightarrow \sigma_{\text{SiC}}^*$ hyperconjugation further promotes the remarkably open Si–O–Si bending angles that are anticipated (in the light of well-known electronegativity differences) by Bent's rule. The resultant softening of low-frequency torsional and bending modes (averting the steric “stiffening” effects of permethylation in

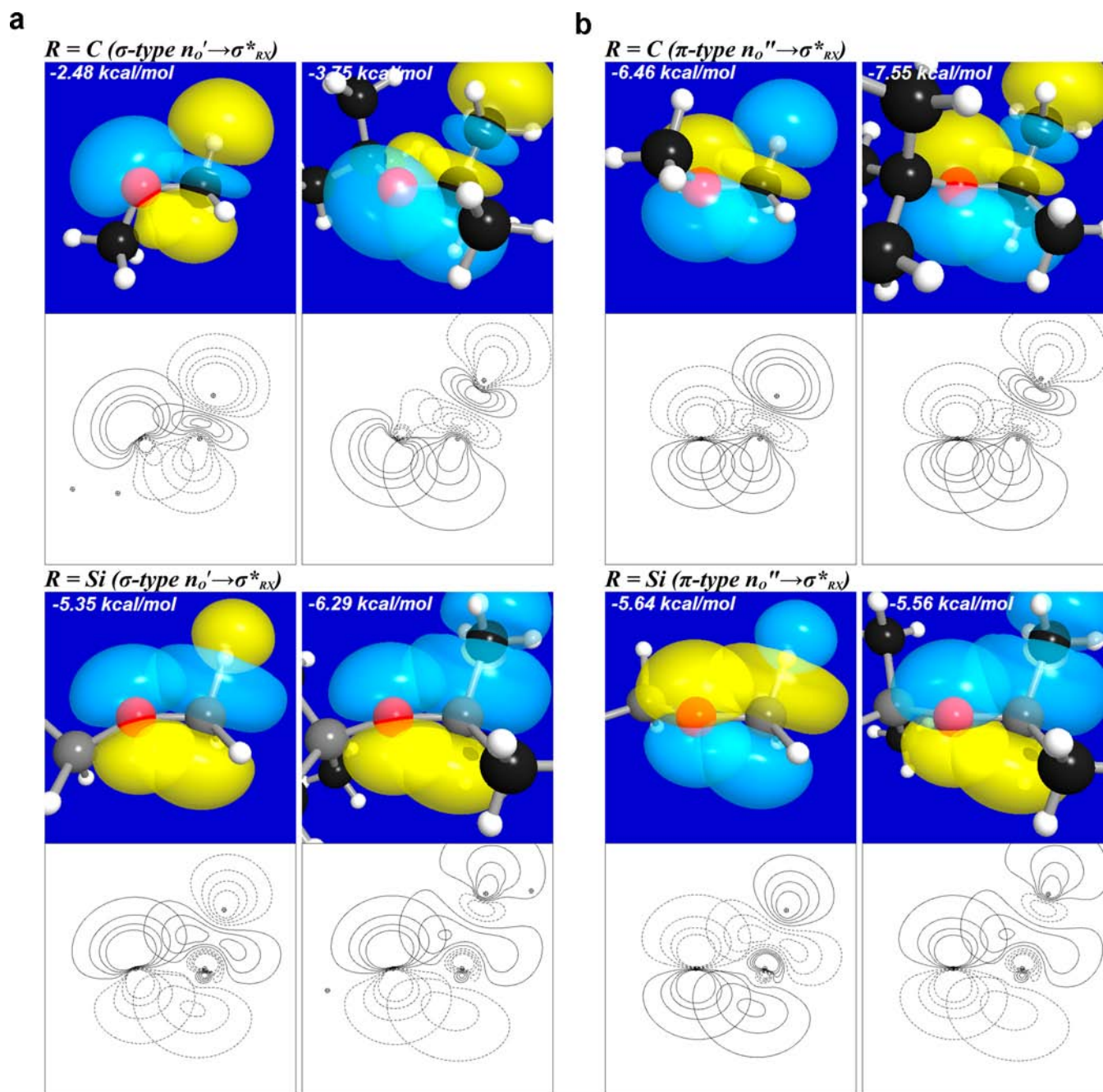


Figure 3. (a) Vicinal σ -type $n_{O'} \rightarrow \sigma_{RX}^*$ hyperconjugative interactions (and associated $E^{(2)}$ stabilization energy; cf. Table 3) in ethers (upper) and siloxanes (lower), as compared in surface and contour plots. (b) Similar to Figure 3a, for vicinal π -type $n_{O''} \rightarrow \sigma_{RX}^*$ hyperconjugative interactions.

ethers) confers an important entropic advantage that further enhances the thermal stability of HMDSE and related silicone polymers.

The present study also re-emphasizes the importance of hyperconjugative (resonance-type) aspects of basicity and hydrogen bonding, in contrast to the superficial “electrostatic” or “dipole–dipole” models widely promoted in current textbooks.³¹ The intrinsic competition in general $(X_3Si)_2O \cdots HA$ interactions between intra- vs intermolecular hyperconjugation ($n_{O'} \rightarrow \sigma_{SiX}^*$ vs $n_{O'} \rightarrow \sigma_{AH}^*$ interactions) virtually dictates the weakened basicity of siloxanes, despite the nearly two-fold increase in oxygen anionicity compared to ethers. Our results reinforce the sharp challenges that silicones present to current electrostatics-based conceptions (and

molecular dynamics “simulations”) of H-bonding and related intermolecular phenomena.

■ ASSOCIATED CONTENT

📄 Supporting Information

This material is available free of charge via the Internet at <http://pubs.acs.org>.

■ AUTHOR INFORMATION

Corresponding Author

west@chem.wisc.edu

Notes

The authors declare no competing financial interest.

ACKNOWLEDGMENTS

We thank Milo Westler of UW-Biochemistry NMRFAM for computational assistance.

REFERENCES

- (1) Burkhard, J. *Chemistry and Technology of Polysiloxanes*. In *Silicones: Chemistry and Technology*; CRC Press: Boca Raton, 1991; pp 21–23.
- (2) Pawlenko, S. *Organosilicon Chemistry*; de Gruyter: Berlin, 1986; pp 43–62.
- (3) Weinhold, F.; West, R. *Organometallics* **2011**, *30*, 5815–5824.
- (4) Baney, R. H.; Lake, K. J.; West, R.; Whatley, L. S. *Chem. Ind.* **1959**, 1129–1130.
- (5) West, R.; Whatley, L. S.; Lake, K. J. *J. Am. Chem. Soc.* **1961**, *83*, 761–764.
- (6) West, R.; Wilson, L. S.; Powell, D. L. *J. Organomet. Chem.* **1979**, *178*, 5–9.
- (7) C. Laurence, C.; Graton, J.; Berthelot, M.; Bessau, F.; Le Questell, J.-Y.; Lucon, M.; Ouvrard, C.; Planchat, A.; E. Renault, E. *J. Org. Chem.* **2010**, 4105–4123.
- (8) Cypriak, M.; Apeloig, Y. *Organometallics* **1997**, *16*, 5938–5949.
- (9) C. G. Pitt, C. G.; Bursey, M. M.; Chatfield, D. A. *J. Chem. Soc., Perkin Trans. 2* **1976**, 434–438.
- (10) Bock, H.; Mollere, P.; Becker, G.; Fritz, G. *J. Organomet. Chem.* **1973**, *61*, 113.
- (11) Shambayati, S.; Schreiber, S. L.; Blake, J. F.; Wierschke, S. G.; Jorgenson, W. L. *J. Am. Chem. Soc.* **1990**, *112*, 697–703.
- (12) Shepherd, B. D. *J. Am. Chem. Soc.* **1991**, *113*, 5581–5583.
- (13) Gillespie, R. J.; Johnson, S. A. *Inorg. Chem.* **1997**, *36*, 3031–3039.
- (14) Grabowsky, S.; Hesse, M. F.; Paulmann, C.; Luger, P.; Beckmann, J. *Inorg. Chem.* **2009**, *48*, 4384–4393.
- (15) For overviews of NBO theory and applications, see: (a) Weinhold, F. *Natural Bond Orbital Methods*. In *Encyclopedia of Computational Chemistry*; Schleyer, P. v. R., Allinger, N. L., Clark, T., Gasteiger, J., Kollman, P. A., Schaefer, H. F., III, Schreiner, P. R., Eds.; John Wiley & Sons: Chichester, 1998; Vol. 3, pp 1792–1811; (b) Glendening, E. D.; Landis, C. R.; Weinhold, F. *WIREs Comput. Mol. Sci.* **2012**, *2*, 1–42. (c) Weinhold, F., Landis, C. R. *Valency and Bonding: A Natural Bond Orbital Donor-Acceptor Perspective*; Cambridge University Press: Cambridge, 2005. (d) Weinhold, F., Landis, C. R. *Discovering Chemistry with Natural Bond Orbitals*; Wiley-Interscience: Hoboken, 2012. (e) See also background and tutorial links on the NBO website: www.chem.wisc.edu/~nbo5.
- (16) Badenhop, J. K.; Weinhold, F. *J. Chem. Phys.* **1997**, *107* (5406–5421), 5422–5432.
- (17) ref 15c, pp. 30–32.
- (18) Chernega, A. N.; Antipin, M. Yu.; Struchkov, Yu. T.; Nikson, D. *F. Ukrain. Khim. Zh.* **1993**, *59*, 196–200.
- (19) Csakvari, B.; Wagner, Z.; Gomori, P.; Mijhoff, F. C.; Rozsondai, B.; Hargittai, I. *J. Organomet. Chem.* **1976**, *107*, 287–294.
- (20) Borisenko, K. B.; Rozsondai, B.; Hargittai, I. *J. Mol. Struct.* **1997**, *406*, 137–144.
- (21) Carteret, C.; Labrosse, A. *J. Raman Spectrosc.* **2010**, *41*, 996–1004.
- (22) Liedle, S.; Mack, H.-G.; Oberhammer, H.; Imam, M. R.; Allinger, N. L. *J. Mol. Struct.* **1989**, *198*, 1–15.
- (23) Allinger, N. L.; Chen, K.-H.; Lü, J.-H.; Durkin, K. A. *J. Comput. Chem.* **2003**, *24*, 1447–1472.
- (24) Gregerson, L. N.; Siegel, J. S.; Baldridge, K. K. *J. Phys. Chem. A* **2000**, *104*, 11106–11110.
- (25) Tamagawa, K.; Takemura, M.; Konaka, S.; Kimura, M. *J. Mol. Struct.* **1984**, *125*, 131–142.
- (26) ref 15d; Table 4.2.
- (27) Bent, H. A. *Chem. Rev.* **1961**, *61*, 275–311. Bent, H. A. *J. Chem. Educ.* **1960**, *37*, 616–634. ref 15c; pp. 138ff and 421ff. For computational evidence of this effect in Si–O–Si bonding, see Schleyer, P. v. R. *Pure Appl. Chem.* **1987**, *59*, 1647.
- (28) Coulson, C. A. *Valence*, 2nd ed.; Oxford University Press: London, 1952; Chap. 8. Ref 15c; p 107ff.
- (29) Reed, A. E.; Curtiss, L. A.; Weinhold, F. *Chem. Rev.* **1988**, *88*, 899–926. Note that the parallels between intra- ($n_{\text{O}} \rightarrow \sigma_{\text{RX}}^*$) vs intermolecular ($n_{\text{O}} \rightarrow \sigma_{\text{AX}}^*$) donor–acceptor delocalizations are so strong that the latter are now commonly considered as “hyperconjugative” phenomena [see Alabugin, I. V.; Gilmore, K. M.; Peterson, P. W. *Wiley Interdisciplinary Reviews: Computational Molecular Science* **2011**, *1*, 109–141. Grabowski, S. J. *Chem. Rev.* **2011**, *111*, 2597–2625]. Strong couplings between such interactions (whether intra- or intermolecular) are therefore to be expected (see ref 15c; p. 693ff).
- (30) As noted in ref 3, this difference in skeletal bond angles is the key factor in enhancing hyperconjugative $n_{\text{O}} \rightarrow \sigma_{\text{RX}}^*$ delocalization in DSEs vs ethers, because at any fixed R–O–R angle the $n_{\text{O}} \rightarrow \sigma_{\text{RX}}^*$ interaction is often found to be stronger for R = C than for R = Si. Aspects of this paradoxical relationship can be exhibited in the present case by considering a simple strained model of HMDME (14.6 kcal/mol above equilibrium) with $\Theta_{\text{COC}} = 156.7^\circ$ (the bond angle of HMDSE), which leads to successive Table 4 entries as follows: 1.932 (occ. n_{O}'), 1.924 (occ. n_{O}''), 0.144 (hc loss), 27.4% (rel. %), –4.83 [$E^{(2)}(n_{\text{O}}' \rightarrow \sigma_{\text{RX}}^*)_{\text{max}}$], –17.54 [$n_{\text{O}}' \rightarrow \sigma_{\text{RX}}^*$], –7.50 [$E^{(2)}(n_{\text{O}}'' \rightarrow \sigma_{\text{RX}}^*)_{\text{max}}$], –23.50 [$E^{(2)}(n_{\text{O}}'' \rightarrow \sigma_{\text{RX}}^*)_{\text{total}}$]. Thus, the total hyperconjugative stabilizations of HMDSE vs strained HMDME are estimated to be very similar (–41.94 vs –41.04 kcal/mol), and that for strained HMDME would likely increase upon relaxation of remaining geometrical variables.
- (31) Textbook definitions of H-bonding are highly conserved between successive editions and tend to employ near-identical verbiage in support of the classical electrostatic “dipole–dipole” viewpoint, viz., “a type of dipole–dipole interaction”: Brown, T. E.; LeMay, H. E. H.; Bursten, B. E.; Murphy, C.; Woodward, P. *Chemistry: The Central Science*, 12th ed.; Prentice Hall: Upper Saddle River, NJ, 2012; p 432; “a special type of dipole–dipole interaction”: Burdge, J. *Chemistry*, 2nd ed.; McGraw-Hill: Boston, 2011; p 495; “particularly strong dipole–dipole forces”: Zumdahl, S. S.; Zumdahl, S. A. *Chemistry: An Atoms First Approach*; Brooks Cole: Belmont, CA, 2012; p 329; “an extreme form of dipole-dipole interaction”: Kotz, J. C.; Treichel, P. M.; Townsend, J. R. *Chemistry and Chemical Reactivity*, 7th ed.; Brooks Cole: Belmont, CA, 2009; p 562; “especially enhanced dipole–dipole forces”: Siska, P. *University Chemistry*; Prentice-Hall: Upper Saddle River, NJ, 2005; p 500; “a special kind of dipole-dipole force”: Moore, J. W.; Stanitski, C. L., Jurs, P. C. *Chemistry: The Molecular Science*, 4th ed.; Brooks Cole: Belmont, CA, 2010; p 406; “a sort of super dipole-dipole force”: Tro, N. J. *Chemistry: A Molecular Approach*, 2nd ed.; Prentice-Hall: Boston, 2011; p 464, and many similar. For considerable evidence supporting the opposed view that resonance-type hyperconjugative (“charge transfer”) interactions are the dominant contribution to H-bonding, see: Weinhold, F.; Klein, R. A. *Mol. Phys.* **2012**, *110*, 565–579.